NEW DIFFERENTIAL DATA ANALYSIS METHOD IN THE ACTIVE THERMOGRAPHY.

J. Rumiński, M. Kaczmarek, A. Nowakowski
Department of Medical and Ecological Electronics, Technical University of Gdańsk, Gdańsk, Poland

Abstract - **A new method for parametric images synthesis in active thermography is proposed. Basing on experimental results the thermal model of an observed object is defined. Images of reconstructed model parameters are formed allowing clear visualization of object thermal properties. Studies made on phantoms and *in-vivo* measurements are presented. Possible applications of the method are discussed**.

Keywords **- Active thermography, image synthesis, parametric imaging**

I. INTRODUCTION

During the last decades of the XX-th century different methods to enhance quality of thermal images or to create quantitative detection rules for medical diagnosis were proposed. For example application of microwave irradiation may improve contrast in tumor detection [1]. Introduction of statistical description and differential analysis of thermal image regions [2] has significant practical value. Detecting of physiological function changes from time sequential thermal images of skin surface is also possible as it was proposed in [3]. In parallel to classical thermography new dynamic measurement techniques were developed for non-destructive testing and evaluation (NDT/NDE) [4] indicating possibility of medical applications [5]. Here a new method for parametric images synthesis in active thermography is described. Some results of phantom and *in-vivo* studies are presented.

II. METHODOLOGY

In active thermography external or internal excitations are applied to an object to modify it's temperature distribution. Measurements of temperature during and/or after the excitation produce data which can be processed to extract information about dynamic properties of the object. In pulsed thermography, used in the reported study, a target object is excited during a given time period t_1

$$U_P(t) = A*\left(\Phi(t) - \Phi(t-t_1)\right), \qquad (1)$$

where: A – amplitude of the excitation, $\Phi(t)$ - Heaviside, step function. Depending on a source of excitation the object temperature increases (heating – e.g. optical source) or decreases (cooling – e.g. a fan or an air conditioner). As it was analyzed by Buettner [6] temperature decrease of human tissues after removal of a heating source is described by a sum of exponents. Exponential character of temperature changes is also valid for cooling object using forced convection. In our studies we focus on optical sources as well as on forced convection generators since they are cheap and simple to use. Let's assume that temperature of a single point of an object can be measured over a given time period t what is represented by a set of samples

$$S_c^p = \left\{ s_1^p, s_2^p, s_2^p, .., s_c^p \right\}, \qquad (2)$$

where: c – total number of samples measured after removal of a heating source or during forced convection cooling, p – index of a measurement point.

Applying exponential model for thermal transients of the object the estimate of a sample is given by

$$\hat{s}_i^p = B_0^p + \sum_{l=1}^{L} B_l^p * \exp\left(-\frac{t_i}{\tau_l^p}\right), \mathrm{i} = 1..\mathrm{c}, \qquad (3)$$

where: B_0^p - an offset, L – a number of exponents in the model (or number of layers in the equivalent electrical RC circuit), B_l^p and τ_l^p – a set of parameters for each exponent (layer), t_i - measurement time.

Parameters of the model can be determined using one of curve fitting methods, assuming given value of the fitting error ε

$$\left| s_1^p - \hat{s}_1^p \right| < \varepsilon . \qquad (4)$$

In the reported studies we used the Marquardt method with the modification given by Bevington [7].

As a result of the fitting procedure a set of model parameters is created for any of simultaneously measured object points forming new parametric images. The number of useful parametric images depends on the object structure and measurement accuracy. In our studies one and two exponential models equivalent to one and two physical layers are sufficient (A1= B_1^p, A2=1/τ_1^p, A3= B_2^p, A4=1/τ_2^p).

Synthesis of parametric images in active thermography is useful only if new information is carried on by those images, or if there is an enhancement of contrast, comparing to traditional thermograms. The validity of the proposed method is tested basing on experiments and on simulations.

Simulation based verification of the proposed method has been done using Finite Element Method heat-flow modeling. As an object a uniform cylinder has been created (diameter 20cm, depth 7 cm) with embedded in the center small cylinder (diameter 4cm, depth 2 cm). About 5000 elements were used to compose the object. The object was heated during 30 s with the radiant flux 2000 (W/m).

Experimental verification of the method was performed on phantoms and *in-vivo*. In the applied pulsed thermography the optical heating excitation was usually lasting 30s. The thermal camera, Agema Thermovision 900, was placed 55 cm far from a target object. The thermal response was measured after excitation of the object by a thermal pulse

Report Documentation Page

Report Date	Report Type	Dates Covered (from... to)
25OCT2001	N/A	-

Title and Subtitle New Differential Data Analysis Method in the Active Thermography	**Contract Number**
	Grant Number
	Program Element Number
Author(s)	**Project Number**
	Task Number
	Work Unit Number
Performing Organization Name(s) and Address(es) Department of Medical and Ecological Electronics, Technical University of Gdañsk, Gdañsk, Poland	**Performing Organization Report Number**
Sponsoring/Monitoring Agency Name(s) and Address(es) US Army Research, Development & Standardization Group (UK) PSC 802 Box 15 FPO AE 09499-1500	**Sponsor/Monitor's Acronym(s)**
	Sponsor/Monitor's Report Number(s)

Distribution/Availability Statement
Approved for public release, distribution unlimited

Supplementary Notes
Papers from the 23rd Annual International Conference of the IEEE Engineering in Medicine and Biology Society, 25-28 October 2001, held in Istanbul, Turkey. See also ADM001351 for entire conference on cd-rom., The original document contains color images.

Abstract

Subject Terms

Report Classification unclassified	**Classification of this page** unclassified
Classification of Abstract unclassified	**Limitation of Abstract** UU

Number of Pages
4

generated by a set of lamps (1000W) located 55 cm far from the object surface. Thermal images were captured every 1 s during 120 seconds (120 images) after switching the heat source off. As an image is constructed by a matrix of 204x128 pixels this gives 26112 measurement points for the image.

Different target objects were used in experiments. Some preliminary results on phantoms have been published in [8]. Here results of extended studies on phantoms, and additionally *in-vivo* measurements are discussed. Phantoms were made as gelatine objects (diameter 20cm, depth 7 cm) with some embedded materials as it is presented in figure 1.

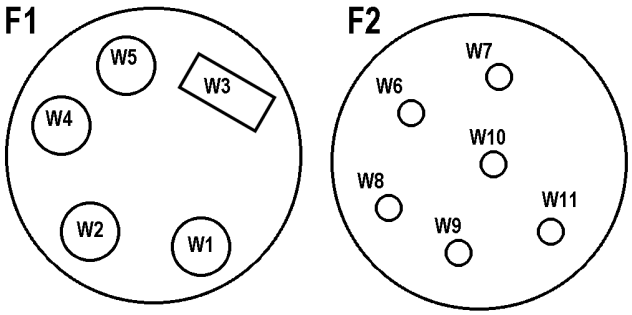

Fig. 1. Two classes of phantoms used in studies.

In the phantom F1 such materials as W1 – silicon, W2 – acryl, W3 – plexiglass, W4 and W5 gelatine with different density were embedded equo-distantly to the gelatine surface. Materials in the second phantom were embedded 3 mm (W6-brass, W8-copper) and 5 mm (W7, W9-aluminum, W10-copper , W11-brass) below the phantom surface.

In-vivo measurements were performed on eight anesthetized pigs according to all procedures accepted by the local Committee of Ethics and Good Practice.

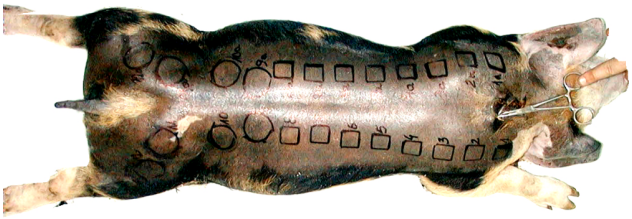

Fig. 2. Pig with indicated burned fields.

Symmetric injuries on the pig skin were generated using preheated burning tools of controlled temperature which were applied during a given period of time. Depth of resulting burns was evidenced by histopathologic evaluation as it is presented in [9]. Placement of burns is shown in Fig. 2.

III. Results

Results of simulations performed for materials as used in the phantom F1 clearly indicate differences in proposed parameters values (Fig. 3). For the 1-exponent model a high correlation between values of the parameter A2 calculated for the simulated and for the measured data exists. In repeatable experiments the maximal deviation between those values is lower than 6%. For the 2-exponent model high

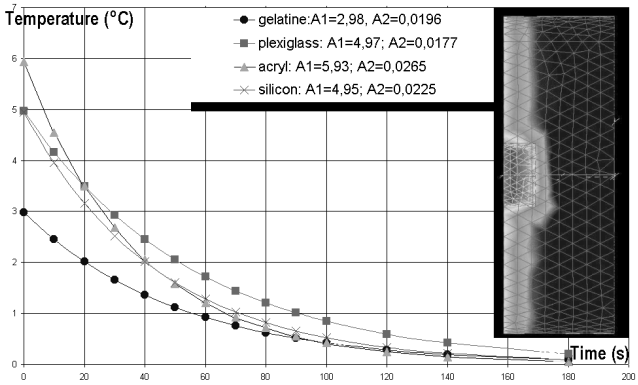

Fig. 3. Simulation results: Temperature decrease of the phantom F1 materials - 1-layer model parameters. Temperature distribution in the phantom 120 s after heating was switched off is presented.

differences (5-10 times) are observed for A2 parameter values for each of exponents. Big differences exist for each of exponents. Such big differences are expected according to the equation of temperature decrease after removal of the heating source, presented by Buettner [6]

$$T(0,t) = To + Ti \cdot \sum_{n=1}^{\infty} e^{-u\cdot(2n+1)^2} / (2n+1)^2 \ , \qquad (5)$$

where: $u = \frac{k}{\rho \cdot C} \cdot \frac{\pi^2}{4 \cdot d^2} \cdot t$; (6)

k – thermal conductivity; $\rho \cdot C$ -volumetric heat capacity; d – depth, for boundary conditions

x = d; t = 0; T > To; (7)

x ≤ d; t = 0; T = To+Ti(1-x/d).

Basing on this formula and on our results it can be stated that for current measurement accuracy in thermography the 2-layer model is sufficient to represent measured data. If temperature changes introduced by an excitation source in the object are high enough then the 2-layer model estimation is better correlated to the measured data comparing to 1-layer model (fig 4).

However, if temperature changes introduced in an object are

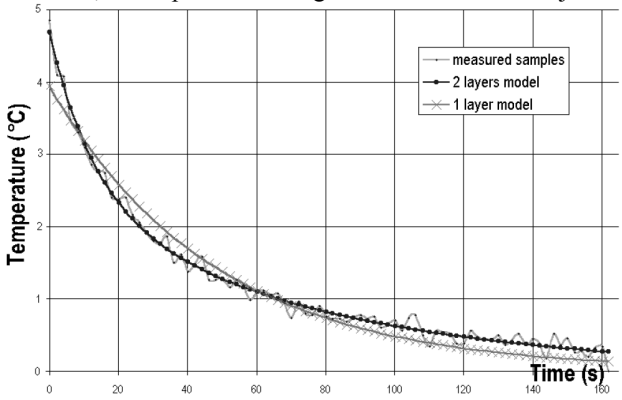

Fig. 4. Differences between 1-exponent and 2-exponent original data estimation.

small the 1-layer model is suitable because the limited measurement accuracy is not allowing for proper

determination of higher order model parameters. In figure 5 an example of traditional (static) thermogram and the A2 parametric image of the phantom F1 are presented. Placements of embedded materials is indicated in fig. 1. In the A2 image W1, W2 and W3 fields are easy to be detected while in the static thermogram only W3 is observed. For the F2 phantom

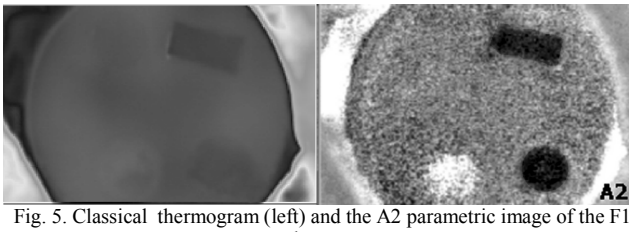

Fig. 5. Classical thermogram (left) and the A2 parametric image of the F1 phantom.

the 2-layer model gives much better results than the 1-layer model. The A4 parametric image (Fig. 6 right) presents all fields with the embedded materials while they are invisible in the thermogram. Even more, it is possible to distinguish between materials embedded closer to the surface (W6, W8) and deeper (other fields).

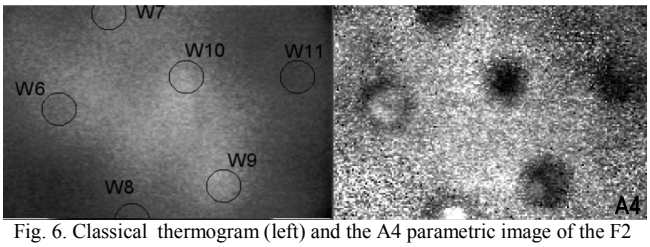

Fig. 6. Classical thermogram (left) and the A4 parametric image of the F2 phantom.

Very interesting results are also obtained for *in-vivo* measurement data. More than 150 measured sequences were processed to create 1-layer and 2-layer parametric images. However because of high fluctuations of the measured signal and small temperature changes in objects, values of the second set of parameters in the 2-layer model were close to zero. Concluding, the 1-layer model seems to be suitable for screening purposes as the following properties has been observed:

- injuries directly caused by the burning tool are characterized by smaller values of A1 and A2 parameters than for the healthy skin (e.g. a black field in fig. 7),
- injuries developed after burning (usually after 10-24 hours) are characterized by higher values of A2 (e.g. white areas in fig. 8), while A1 has different values (smaller and higher than for the healthy skin) depending on the animal.

In the first class of injuries A2 parameter values are below 0.019, usually 0.009. In contrary, for the second class of injuries values of A2 parameters are grater than 0.029. The healthy skin is characterized by A2 parameter values between 0.021 and 0.026. The relation between those injuries and healthy skin properties is shown in figure 9. Evident difference between injuries and healthy skin can be used to

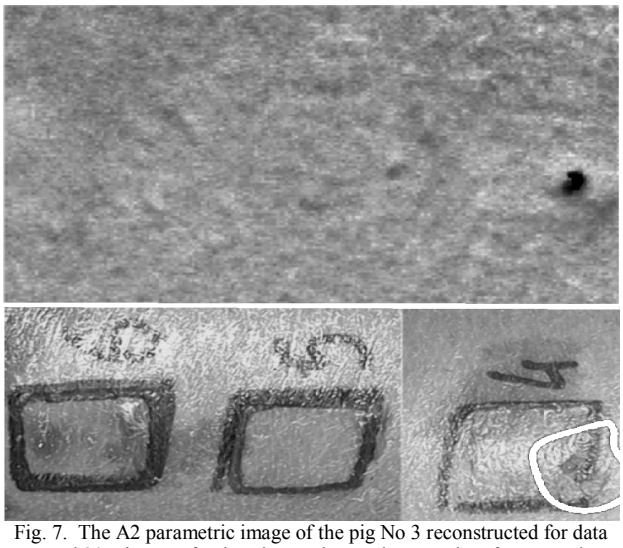

Fig. 7. The A2 parametric image of the pig No 3 reconstructed for data measured 30 minutes after burning. Below a photography of measured area taken at the same time.

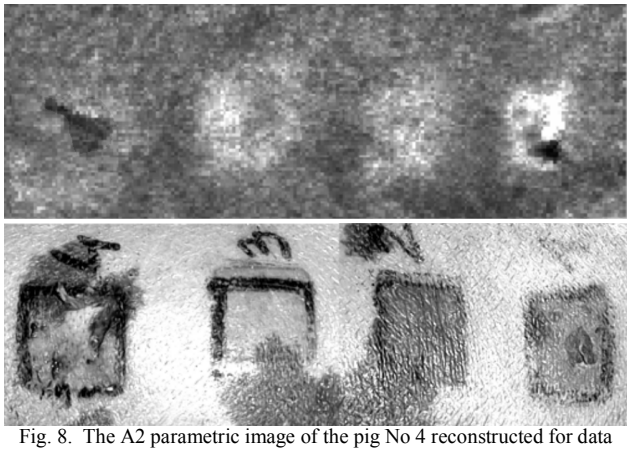

Fig. 8. The A2 parametric image of the pig No 4 reconstructed for data measured 24 hours after burning. Below a photography of measured area taken at the same time.

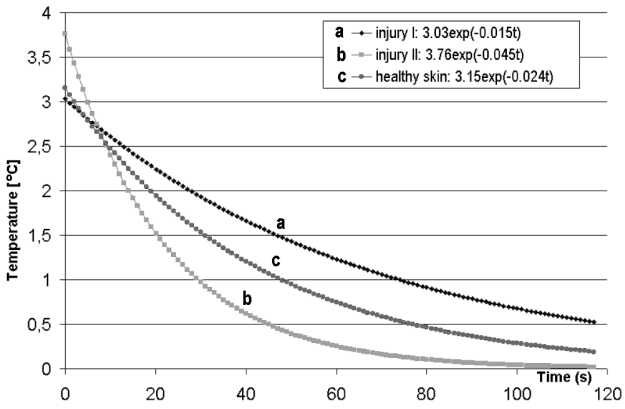

Fig. 8. Characteristics of temperature changes for two classes of injuries and healthy skin.

establish threshold values for the A2 parameter. It is possible then to distinguish automatically specific types of tissue changes. In figure 9 an example of the thresholding operation (threshold=0.031) is presented, applied to the A2 parametric image for data collected from pig No 4, 96 hours after burning. Since A2 parameter values are repeatable and related to thermal properties of the object they can be used in differential analysis within a one image and between different images reconstructed for particular objects.

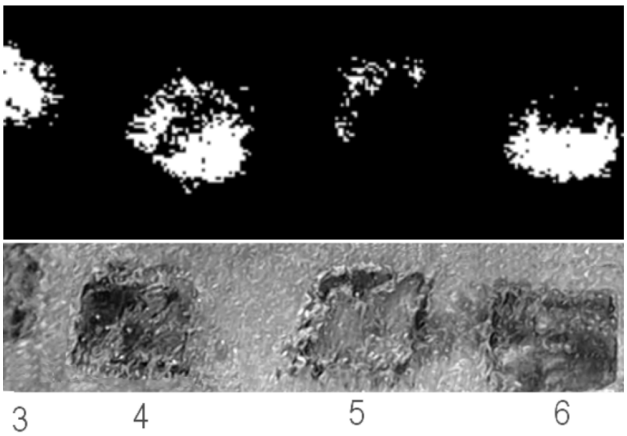

Fig. 9. Binary image of the A2 parameter after thresholding operation (threshold=0.031) applied for data collected from pig No 4, 96 hours after burning. Below a photography of measured area taken at the same time.

Additionally, interesting founding was observed for burned fields generated by high temperature burning tools applied for short time (e.g. the field No 7). In the A2 parameter images they were characterized by a very high value (usually 2-4 times greater than for the healthy skin) in comparison to other fields.

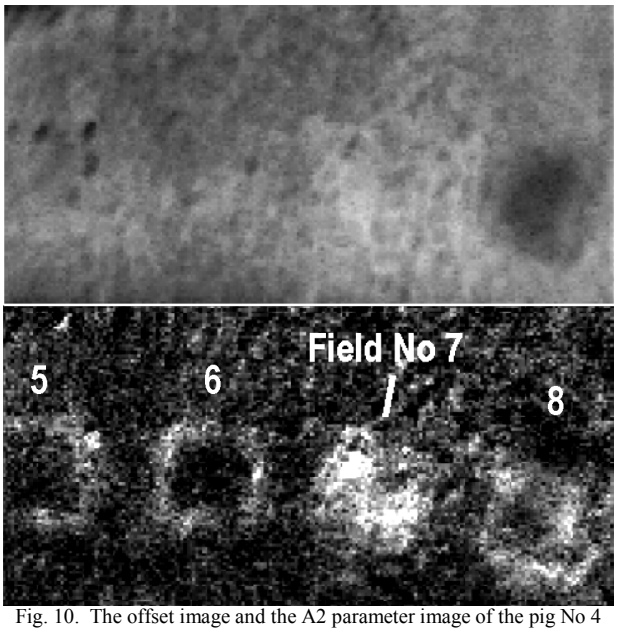

Fig. 10. The offset image and the A2 parameter image of the pig No 4 reconstructed for data measured 48 hours after burning.

IV. Discussion and conclusion

Parametric images synthesized from a sequence of thermograms represent thermal properties of a tested object. Differentiation of specific materials (tissues) is possible using comparison of corresponding τ_l^p parameters. Phantom studies results as well as *in-vivo* results allow to identify such object properties (materials) that are impossible to be indicated with traditional thermography. However further enhancement must be done to the measurement setup. Increase in temperature resolution of a thermal camera and in temperature contrast of an object (improvements in the excitation system) should allow the discrimination of materials with small differences of thermal properties (mainly conductivity). Extended medical investigations must be done to establish calibration procedures for direct determination of the thickness of burned tissues. Other possible applications of the presented method may concern all cases where thermal properties of external tissues are affected, see e.g. [12] for cardiologic cases.

References

[1] Thomson J.E., Simpson T.L., Caulfield J.B.,: Thermographic tumor detection enhancement using microwave heating. *IEEE Trans. on Microwave theory and techniques*, 26 (1978), 573-580.

[2] Mabuchi K., Chinzei T., Fujimasa I., Haeno S., Abe Y., Yonezawa T.: An image-processing program for the evaluation of asymmetrical thermal distributions. *Proc. 19th Int. Conf. IEEE/EMBS*, Chicago, USA, (1997), 725-728.

[3] Fujimasa I., Chinzei T., Mabuchi K., Converting algorithms for detecting physiological function changes from time sequential thermal images of skin surface, *1995 IEEE Engineering in Medicine and Biology,* IEEE. Part vol.2, 1709-10.

[4] Maldague X., Applications of Infrared Thermography in NonDestructive Evaluation, *Trends in Optical Nondestructive Testing*, Pramod Rastogi, (2000), 591- 609.

[5] Rumiński J., Kaczmarek M., Nowakowski A., Hryciuk M., Differential Analysis of Medical Images in Dynamic Thermography. Proc. of the V Conf. on Application of Mathematics in Biology and Medicine, Ustrzyki, Poland, (1999), 126-131

[6] Buettner K., Effects of extrem heat and cold on human skin, *J. Appl. Phys*, 3: 691-713, 1951.

[7] Bevington P.R., Robinson D.K., Data Reduction and Error Analysis for The Physical Sciences, McGraw-Hill Higher Education, 1991.

[8] Rumiński J., Nowakowski A., Kaczmarek M., Model-based parametric images in dynamic thermography, Polish J Med Phys & Eng; 6(3):159-164, 2000.

[9] Kaczmarek M., Nowakowski A., Renkielska A., Grudziński J., Stojek W., Investigation of skin burns basing on active thermography, see the current proceedings.

[10] Nowakowski A., et al., Thermographic and electrical measurements for cardiac surgery inspection, see the current proceedings.